

## Analysis of pile-up/sink-in during spherical indentation for various strain hardening levels

S. Shankar<sup>\*1</sup>, P. Loganathan<sup>2a</sup> and A. Johnney Mertens<sup>1b</sup>

<sup>1</sup>Department of Mechatronics Engineering, Kongu Engineering College, Perundurai, Erode-638052, India

<sup>2</sup>Department of Mechanical Engineering, EBET Group of Institutions, Kangayam-638108, India

(Received August 21, 2013, Revised June 17, 2014, Accepted July 2, 2014)

**Abstract.** The measurement from the indentation process depends on the amount of pile-up or sink-in around the contact impressions. In this paper, finite element concept is utilized to study the pile-up and sink-in behaviour for the wide range of materials with different young's modulus, yield stresses, strain-hardening exponents and co-efficient of friction values. The exact indentation model is created by using the two dimensional axisymmetrical model for simulating the spherical indentation process on the lines of Taljat and Pharr (2004) work. The result shows that during spherical indentation process the amount of pile-up is greatly influenced by the strain hardening exponents in addition to other material properties and depth of penetration. The numerical results from the finite element analysis are also validated using the exact multilinear material properties obtained from the tensile testing for the materials like mild steel, brass and aluminium.

**Keywords:** pile-up; sink-in; indentation; finite element analysis; strain hardening

---

### 1. Introduction

Indentation testing is the process of pressing a highly rigid sphere at a prescribed load into the surface of solid specimen. An indentation process is used to evaluate the material properties such as hardness, elastic modulus, yield strength, strain hardening exponent, fracture toughness, residual stress and creep coefficient which is based on the relationship between the load and displacement. However, the measurement from the indentation process depends on the amount of pile-up or sink-in around the contact impressions. Several researchers reported the amount of pile-up/sink-in for various materials using the experimental and finite element approach. Taljat and Pharr (2004) modeled the spherical indentation process using the finite element concepts and compiled the results for various materials to predict the material pile-up/sink-in. The results were compiled by considering the property of the material as elastic perfectly plastic. Very few materials will exhibit elastic perfectly plastic case; generally there will be some amount of strain hardening in most of the materials.

This paper extends Taljat and Pharr work for various strain hardening levels using the finite

---

\*Corresponding author, Ph.D., E-mail: [shankariitm@gmail.com](mailto:shankariitm@gmail.com)

<sup>a</sup>Ph.D., E-mail: [ploganathanme@gmail.com](mailto:ploganathanme@gmail.com)

<sup>b</sup>P.G., E-mail: [johnneymertens@gmail.com](mailto:johnneymertens@gmail.com)

This paper extends Taljat and Pharr work for various strain hardening levels using the finite element concepts to exactly quantify the material behavior during spherical indentation process on the lines of Shankar and Mayuram (2008) work. The Indentation experimentation process usually relates load, deflection and contact area. Several researches reported their work in the indentation process using the experimental approach. An accurate determination of contact area is made during the measurements of material properties from the indentation process by Oliver and Pharr (1992), and concludes that the hardness and elastic modulus are solely dependent on the contact area. Mesarovic and Fleck (1999) concludes that the indentation is limited by the elastic effects for smaller contacts and contact size which is dependent on the indentation depth. Pharr (1998) emphasis that the hardness and elastic modulus of the material which do not exhibit pile-up that can be measured by nano indentation process and when the pile-up is prevalent, the nano indentation will over estimate the properties by as much as by 50%. Mata and Alcala (2003) concludes that the hardness and surface deformation will remain constant irrespective of applied loading for the given co-efficient of friction. Yueguang and Hutchinson (2003) reported that the parameters such as strain hardening, initial yield strain, indenter geometry and indent size are the important parameters to determine the relationship between the indentation hardness and stress-strain behaviour.

The pile-up and sink-in behaviour of an elastic-plastic material depends on the strain hardening exponent, material properties ( $E/\sigma_y$ ), depth of penetration ( $h/R$ ) and friction co-efficient by Taljat and Pharr (2004). Mostly their results are based on the zero strain hardening, which is typically an elastic perfectly plastic material. Hyungyil *et al.* (2005) concludes that during loading the slope of the loading curves correlates with all material properties, but during unloading the slope is only related with the young's modulus. Chen *et al.* (2005) reported that the yield strength has no effect during the determination of material properties of ceramics using the indentation process. Habbab *et al.* (2006) indicates that the essential parameter which must consider into account is the friction between the contact surfaces during simulation to make an accurate indentation response of a material that pile-up. Hernot *et al.* (2006) concludes that the pile-up behaviour for the spherical indentation is dependent on the material properties and also contact radius during indentation that will be treated as the function of penetration depth. Yan *et al.* (2007) analyzed in super elastic shape memory alloys and reported that the maximum indentation force and unloading slope are not dependent on the reverse transformation stress during the spherical indentation. Kucharski and Mroz (2007) presented a new procedure for determining the plastic stress-strain curve by means of a cyclic spherical indentation testing. Poon *et al.* (2008) concludes that the indenter tip radius is a crucial parameter for determining the accurate elastic properties. Detection of local variation in elastic properties during biological indentation was analysed by Lin *et al.* (2009). Lee *et al.* (2010) determined that the average plastic strain decreases with increasing in hardening and also the strain should be a function of material properties and indentation depth for the spherical indenter.

Overall, the important parameters that the spherical indentation pile-up and sink-in process depends are young's modulus, poisson's ratio, yield strength, depth of penetration, friction coefficient and strain hardening. Taljat and Pharr (2004) considered all the above parameters to model as real indentation process using the finite element concepts for multiple ranges of materials. Since they considered only elastic perfectly plastic material assumption, their analysis fails to cover most of the practical materials. This paper extends Taljat and Pharr (2004) work for multiple range of practical strain hardening values on the lines of Shankar and Mayuram (2008) model to elucidate the difference in the results. Also three different practical strain hardening materials are considered to validate the present finite element results.

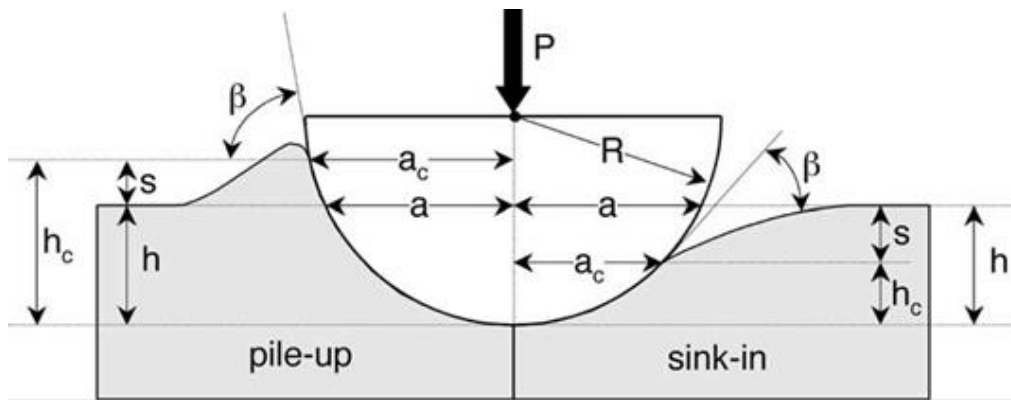


Fig. 1 Spherical indentation contact geometry (Taljat and Pharr 2004)

## 2. Contact geometry

The sink-in to pile-up transition occurs due to the material transformation from the elastic deformation at small depths to the plastic deformation at large depths. The spherical indentation contact geometry is shown in Fig. 1 (Taljat and Pharr 2004) in which a rigid sphere of radius ' $R$ ' penetrates into the material to ' $h$ ' depth due to the driven force ' $P$ '.

The sink-in and pile-up behaviour of a material is shown in right and left side of the Fig. 1. The actual contact depth during pile-up or sink-in behaviour is denoted by ' $h_c$ ' and total indenter penetration depth denoted by ' $h$ '. The symbol ' $a_c$ ' denoted the actual radius of contact and ' $a$ ' denoted surface contact radius i.e., the intersection of indenter with the original undeformed surface. The amount of pile-up or sink-in relative to undeformed surface is denoted by ' $s$ ' and the angle between the tangent line of the contact to the undeformed surface is denoted by ' $\beta$ '. When ' $s$ ' is less than zero sink-in behaviour is dominated and greater than zero the pile-up behaviour will be dominated in the material.

## 3. Finite element simulation

The simulation of the indentation process using the spherical indenter is performed by using ANSYS11<sup>®</sup>. A two dimensional axisymmetric PLANE42 element is selected for the analysis by considering ' $x$ ' coordinate as a radial coordinate ' $r$ ' and ' $y$ ' coordinate as a axial coordinate ' $z$ '. The indenter is modelled as a rigid sphere of radius 10mm and the specimen as a cylinder of 20mm radius and 20mm height as shown in the Fig. 2. The boundary conditions are applied to ensure that there is no displacement in the ' $z$ ' direction and free movements in ' $r$ ' direction. Symmetrical boundary conditions are applied along the centreline and the bottom region is constrained in all directions. The contact between the indenter and specimen is made by fixing the indenter as target surface (rigid surface) and specimen as contact surface by selecting the appropriate coefficient of friction without any initial penetration between the surfaces. The coefficient of friction is selected as 0.2 for most of the computation purpose on the lines of Taljat and Pharr (2004), but limited number of computations is performed using the coefficient of frictions 0.0, 0.1 and 1.0. The non-linear inelastic behaviour such as young's modulus ( $E$ ),

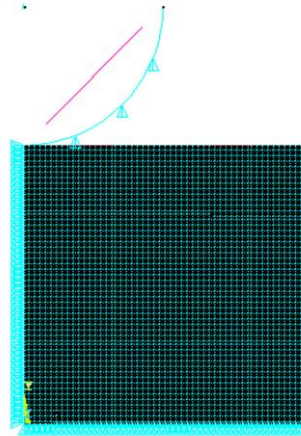
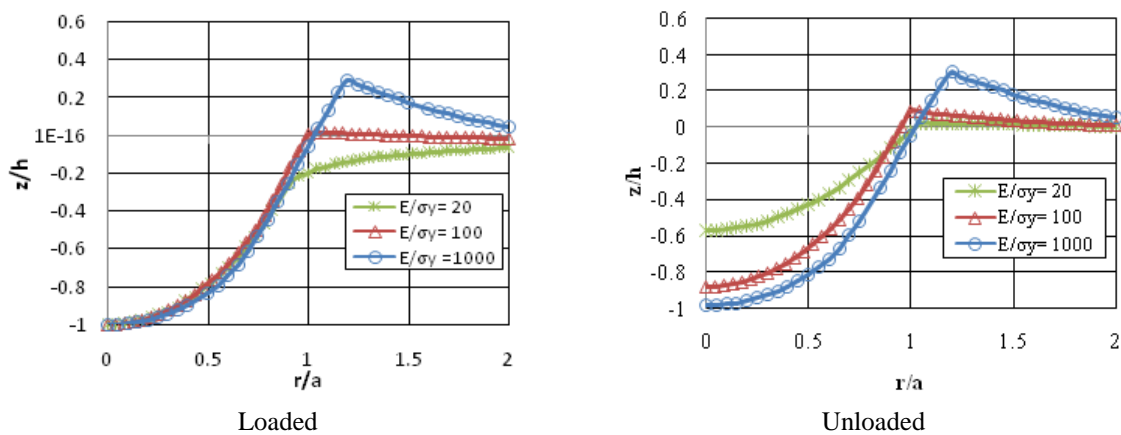


Fig. 2 Finite element meshed model

Fig. 3 Indentation profile for  $h/R=0.2$ ,  $n=0$ , and  $\mu=0.2$ 

poisson's ratio ( $\nu$ ) is assumed and the behaviour is extended to various ranges of yield stress values ( $\sigma_y$ ).

The pile-up and sink-in behaviour is characterized by the depth of penetration ( $h/R$ ) ratio; the ratio of young's modulus to yield stress ( $E/\sigma_y$ ) ratio, the strain hardening exponent/tangent modulus ( $n$ ) and coefficient of friction ( $\mu$ ). To cover a wide variety of material such as metals, ceramics and glasses the values of young's modulus to yield strength is selected from the range 20 to 1000 and also the analysis is extended to various strain hardening exponent values i.e.,  $n$  varies from  $0.0E$ ,  $0.025E$ ,  $0.05E$  and  $0.1E$ . The pile-up and sink-in geometry is examined for both the loading and unloading indentation conditions.

## 4. Result and discussion

### 4.1 Influence of elastic deformation on pile-up

The analysis is carried out initially for several different materials with the elastic perfectly plastic assumption i.e.,  $n=0E$  to validate the Taljat and Pharr (2004) results. The indentation profile for loading as well as unloading using the finite element prediction for various ' $r/a$ ' to ' $z/h$ ' ratios shown in Fig. 3 to the same penetration depth of 0.2 and coefficient of friction 0.2. The material which is used for the investigation are elastic perfectly plastic solid with  $E/\sigma_y$  are 20, 100, and 1000. The sink-in behaviour is observed for the value  $E/\sigma_y=20$  and the material is closer to elastic solid. A small amount of pile-up exhibits for the material having  $E/\sigma_y=100$  and the extensive pile-up occur for the material having  $E/\sigma_y=1000$  as similar to Taljat and Pharr (2004). During unloading, the contact geometry changes due to the elastic recovery. The elastic recovery is large for the material with  $E/\sigma_y=20$  and marginal amount of elastic recovery observed for the material with  $E/\sigma_y=1000$  due to domination of plasticity.

The elastic-plastic behaviour for different strain hardening exponent  $n=0.0E, 0.025E, 0.05E,$  and  $0.1E$  is examined by keeping the  $E/\sigma_y$  values as constant (i.e., 1000 for this case) for various strain hardening exponent values. Fig. 4 shows the loading and unloading behaviour for an elastic-plastic material with  $E/\sigma_y=1000$  ( $\sigma_y=200$  N/mm<sup>2</sup>) with various strain hardening exponents  $n=0.0E, 0.025E, 0.05E, 0.1E$ . The material with  $n=0$  exhibits a pile up behaviour during loaded indentation process while the other three cases with  $n=0.025E, 0.05E$  and  $0.1E$  exhibit sink in behaviour. During unloading, the material loses its elasticity and negligible amount of recovery for the materials is visible as the value of the strain hardening exponent increases. The material is perfectly plastic at  $n=0$ , so pile-up behaviour were dominated. With increase in strain hardening exponent the material has better formability (elastic nature), so sink-in behaviour were dominated.

Fig. 5 shows an elastic/plastic material with  $E/\sigma_y=100$  (i.e.,  $\sigma_y=2000$  N/mm<sup>2</sup>) with various strain hardening exponent values, whose pile up and sink in behaviours are examined during the loaded and unloaded indentation process. From the loaded indentation process, it is found that the material is piling up for  $n=0.0E, 0.025E$  and sinking-in is observed for the materials of  $n=0.05E, 0.1E$ . There is large amount of recovery to elastic state for  $n=0.05E, 0.1E$  and for  $n=0.0E, 0.025E$  recovery of the elastic solid is small during unloading. From the unloaded indentation profile it is evident that the recovery of the material increases with increase in  $n$  and  $E/\sigma_y$  values. That is the reason the graph drops to a lower value than its predecessor when the strain hardening exponent is increased gradually which deteriorates the elastic property of the material. Once the elastic

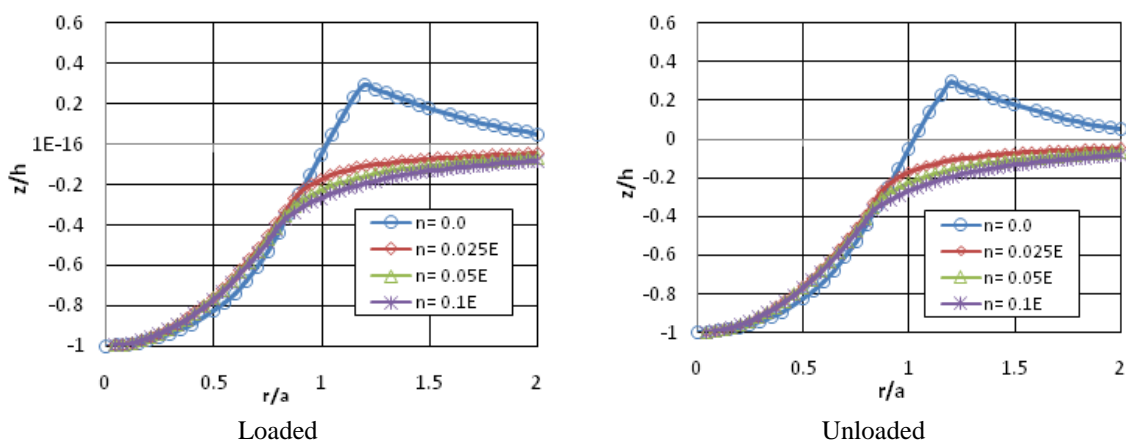
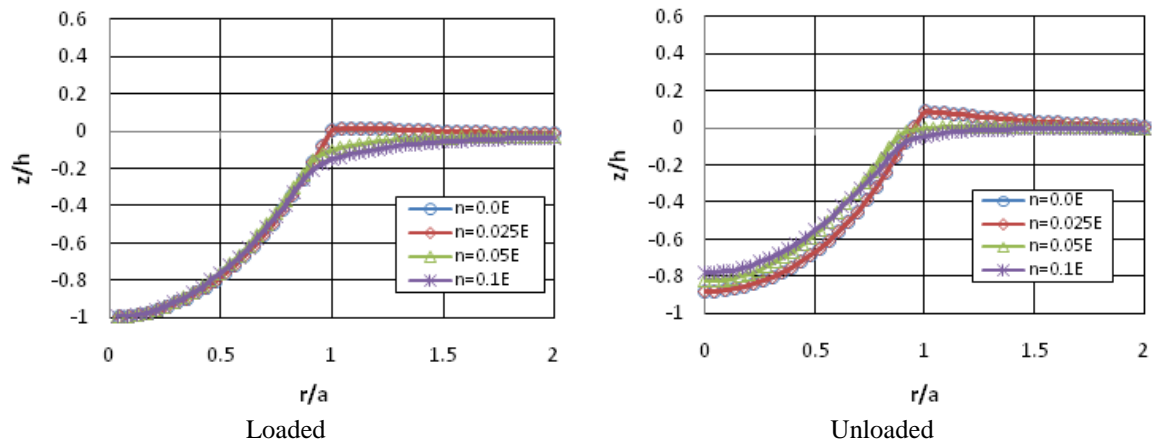
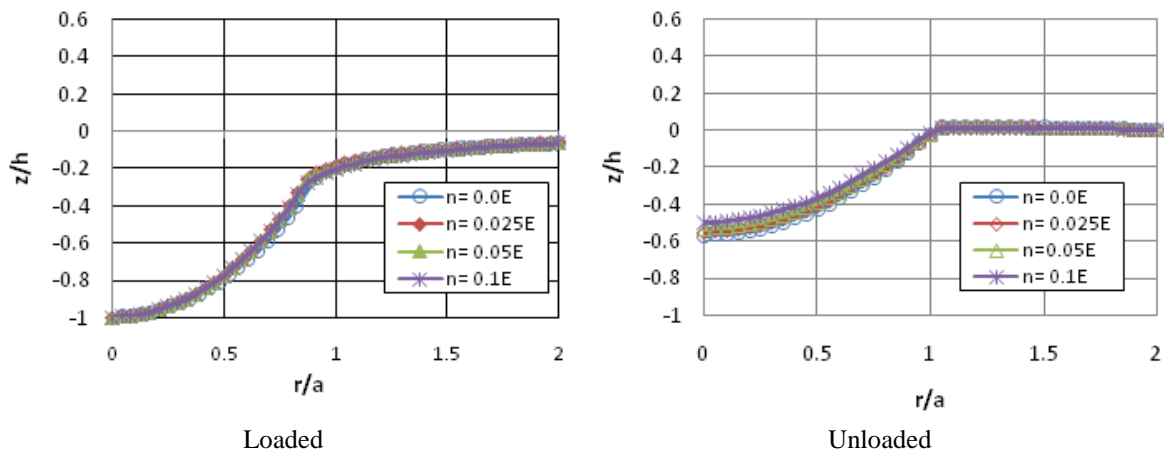


Fig. 4 Indentation profile for strain hardening exponent ( $n$ ) for  $E/\sigma_y=1000$

Fig. 5 Indentation profile for strain hardening exponent ( $n$ ) for  $E/\sigma_y=100$ Fig. 6 Indentation profile for strain hardening exponent ( $n$ ) for  $E/\sigma_y=20$ 

property is lost, the recovery of the material is affected and the deformation is permanent.

The elastic-plastic material with  $E/\sigma_y=20$  with varying strain hardening exponents shown in Fig. 6 and the pile up and sink in behaviours are examined during the loaded and unloaded indentation profile. The magnitudes of sink in obtained for various values of strain hardening exponents are negligible which is evident from the loaded indentation profile. When a material is subjected to small value of yield stress the effect of strain hardening made the material sink-in for all values of  $n$ . The large amount of elastic recovery is observed for all strain hardening exponent ( $n$ ) values at low young's modulus to yield stress ratio. But when the profile is closely observed, the recovery is the maximum for the material with the highest value strain hardening exponent  $n=0.1E$  and the recovery gradually decreases for the materials having the strain hardening exponents  $n=0.05E$ ,  $0.025E$ ,  $0.0E$  respectively. It is inferred from the profile that as the value of strain hardening exponent increases the recovery of the material also increases.

Collectively analysing all the loaded indentation profiles obtained for the various strain hardening exponents for each ( $E/\sigma_y$ ) value, the tendency to pile up decreases as the ( $E/\sigma_y$ ) of the

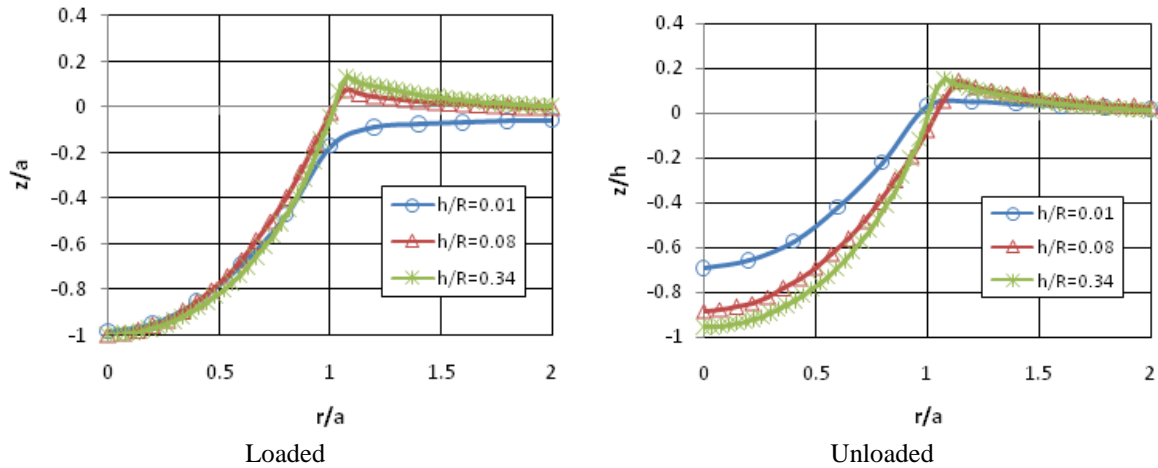


Fig. 7 Indentation profile for  $E/\sigma_y=200$ ,  $n=0$  and  $\mu=0.2$

material decreases. For the material with  $E/\sigma_y=1000$ , extensive pile up is seen, while the material with  $E/\sigma_y=100$  exhibits considerable pile up behaviour and when the material subjected to  $E/\sigma_y=20$ , the effect of sink in is more dominant. From the unloaded indentation profiles, the recovery tends to be more for material with a lower value of  $E/\sigma_y$ . The material which is subjected to  $E/\sigma_y=1000$  shows almost no recovery at all during the unloading phase of the indentation process. In comparison, the material with  $E/\sigma_y=100$  shows a better recovery and the material subjected to yield stress  $E/\sigma_y=20$  shows a large amount of recovery.

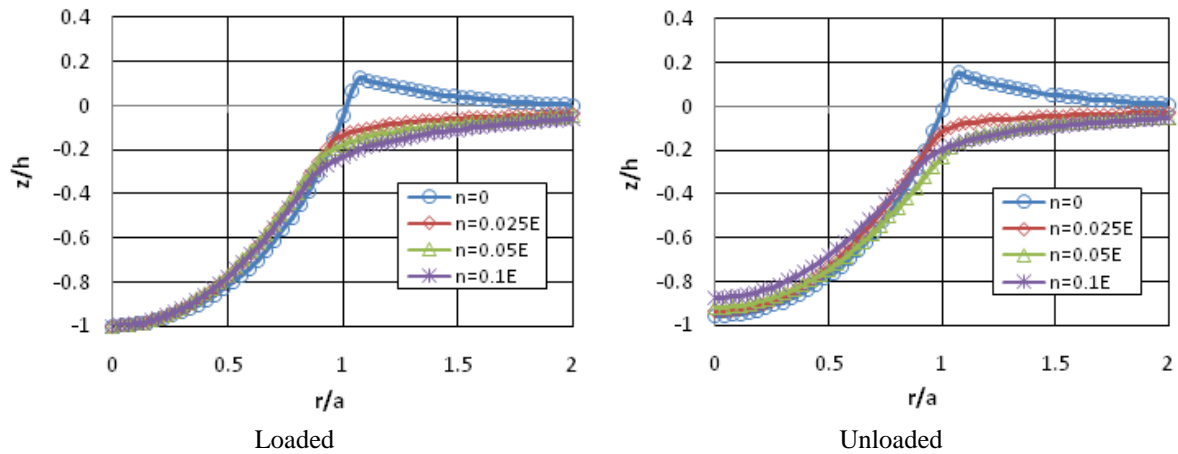
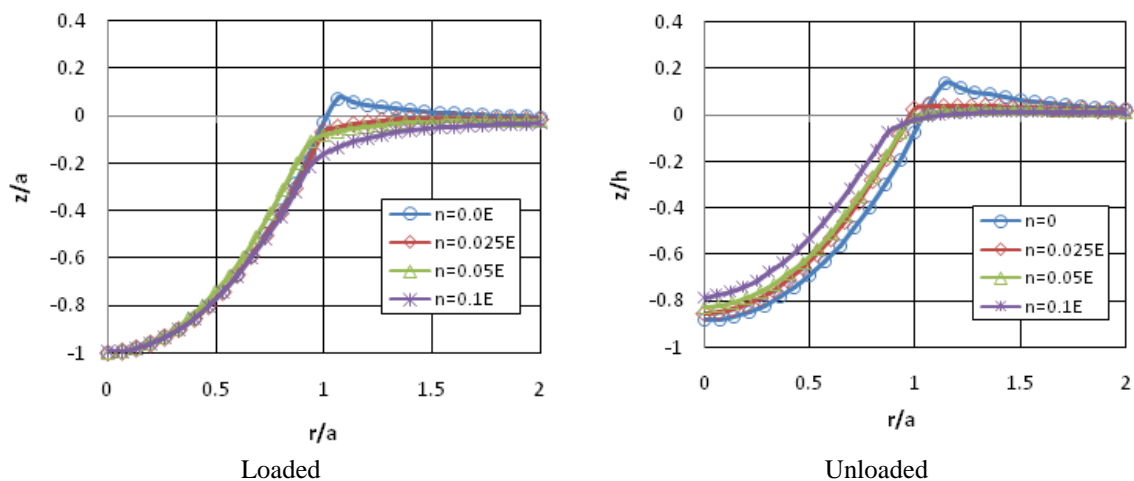
#### 4.3 Influence of penetration depth on pile-up

Fig. 7 shows the depth of penetration which affects the pile up and sink in behaviour for the material with zero strain hardening exponent for the yield stress  $E/\sigma_y=200$ . The loading and unloading indentation profile is obtained by keeping the coefficient of friction as  $\mu=0.2$ .

This simulation is carried out for different penetration depths by keeping the strain hardening exponent ( $n$ ) as constant. For the depth of penetration  $h/R=0.01$  it exhibits sink in behaviour and as the value of penetration depth increases through  $h/R=0.08$  and  $h/R=0.34$ , the pile up behaviour becomes predominant respectively. This is evident from the profile obtained from the simulation that, with the increase in penetration depth piling up of the material escalates. From unloading, the recovery of the material decreases as the penetration depth increases. The recovery is more when the penetration depth is less and hence the elastic property is preserved. While the deformation is more for a material whose depth of penetration is more and hence loses its elasticity.

#### 4.4 Influence of penetration depth and strain hardening on pile-up

The behaviour of elastic-plastic penetration depth for different strain hardening exponents are examined by keeping  $E/\sigma_y$  values as constant. Fig. 8 shows the pile up and sink in behaviour depends on the depth of penetration ( $h/R$ ) by varying the strain hardening exponents  $n=0.0, 0.025, 0.05, 0.1E$  for the material with  $E/\sigma_y=200$ . The loading and unloading indentation profile is obtained with same co-efficient of friction  $\mu=0.2$ . This simulation is carried out for the normalized

Fig. 8 Indentation profile for  $E/\sigma_y=200$ ,  $h/R=0.34$  and  $\mu=0.2$ Fig. 9 Indentation profile for  $E/\sigma_y=200$ ,  $h/R=0.08$  and  $\mu=0.2$ 

penetration depth ( $h/R=0.34$ ) by varying the strain hardening exponent ( $n$ ). With the increase in strain hardening exponent, the sink in behaviour is observed. From the loaded indentation profile of  $h/R=0.34$ , by varying the strain hardening exponent ( $n$ ), the pile-up and sink in behaviours are measured.

In loaded indentation profile, for  $n=0.0E$  the material exhibits pile-up behaviour and for  $n=0.025E$ ,  $0.05E$ ,  $0.1E$  the sink in behaviour is observed indicating that the sink in behaviour dominates over pile up as the value of strain hardening exponent of the material increases. During unloading a large amount of recovery in the material with  $n=0.025E$ ,  $0.05E$ ,  $0.1E$  is visible and the recovery is small for  $n=0.0E$ . Thus the recovery of the material improves gradually with the increase in the value of strain hardening exponent ( $n$ ).

Fig. 9 shows the loaded and unloaded indentation profile by varying the strain hardening exponent for the material with  $E/\sigma_y=200$ , coefficient of friction 0.2 with  $h/R=0.08$ . From the loaded indentation profile, it is evident that the tendency to sink in increases with increase in the value of

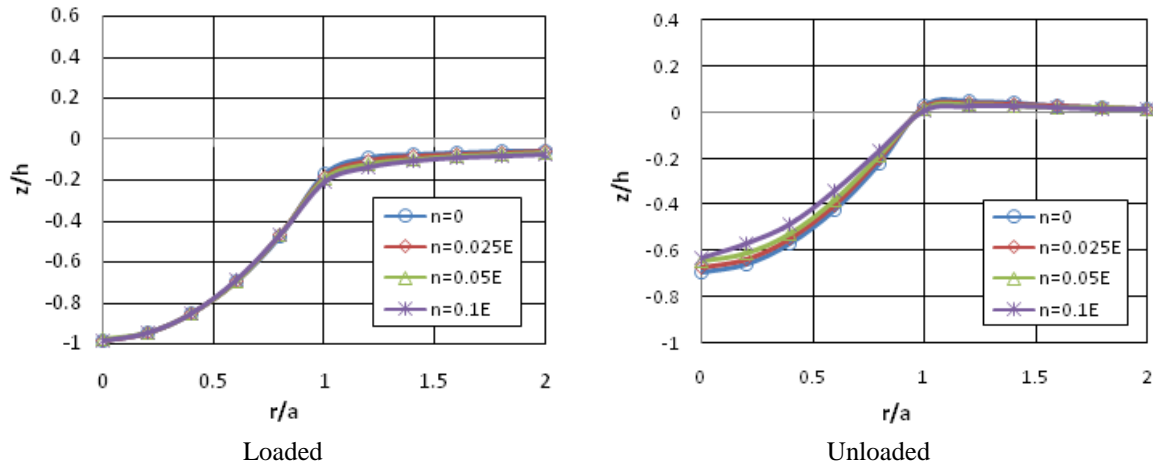


Fig. 10 Indentation profile for  $E/\sigma_y=200$ ,  $h/R=0.01$  and  $\mu=0.2$

strain hardening ( $n$ ) exponent of the material. From the unloaded indentation profile the recovery is largely dependent on the strain hardening exponent ( $n$ ), for the material as the recovery increases with increase in ‘ $n$ ’ value of the material. Hence proves that the material with higher ‘ $n$ ’ value exhibits more elasticity in comparison with a material having lesser ‘ $n$ ’ value.

From Fig. 10, the loaded and unloaded indentation profile were studied by varying the strain hardening exponent for the material with  $E/\sigma_y=200$  and coefficient of friction 0.2 with  $h/R=0.01$ . During loading, the indentation sink in behaviour is observed for all strain hardening exponent ( $n$ ) values. The change in value of strain hardening exponent ( $n$ ) does not affect the sink in behaviour very much and hence the difference between the magnitudes of sink in is negligible for the various materials subjected to the indentation process. This is probably due to the very low depth of penetration value and hence the loaded profiles obtained are similar. During unloading, there is a large amount of recovery in the material for all strain hardening exponents ( $n$ ). The more the value of ‘ $n$ ’, the recovery of the material is also more.

From the loaded indentation profiles obtained for various values of penetration depths the behaviour of pile up changes respect to the depth of penetration values ( $h/R$ ). When the value of penetration depth of a material is large ( $h/R=0.34$ ), the amount of pile up obtained is also high, but as the value of penetration depth decreases to  $h/R=0.08$  and further down to  $h/R=0.01$ , the level of pile up decreases considerably and the sink in behaviour takes over thus showcasing the effect of change in penetration depth. The unloaded indentation profiles signify the recovery of the material which varies with change in the values of penetration depths. This is evident from the unloading indentation profiles which have the penetration depths of  $h/R=0.34, 0.08, 0.01$ . When the value of penetration depth is high ( $h/R=0.34$ ), the recovery is lesser, when the depth of penetration value decreases to  $h/R=0.08$  the recovery is much better and the material with a penetration depth value of  $h/R=0.01$  has the best recovery. Hence, the amount of recovery is not only dependent on the strain hardening exponent ( $n$ ) but also the penetration depth ( $h/R$ ) of the material.

#### 4.5 Effects of contact friction on pile up

The effect of contact friction on pile up is also studied which is obtained as a result of

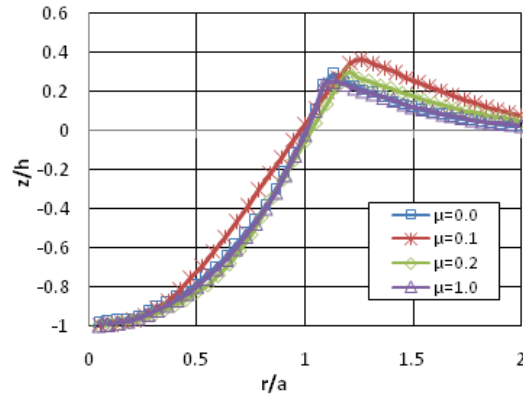


Fig. 11 Effect of contact friction on the loaded indentation profile for  $h/R=0.2$ ,  $E/\sigma_y=1000$  and  $n=0$

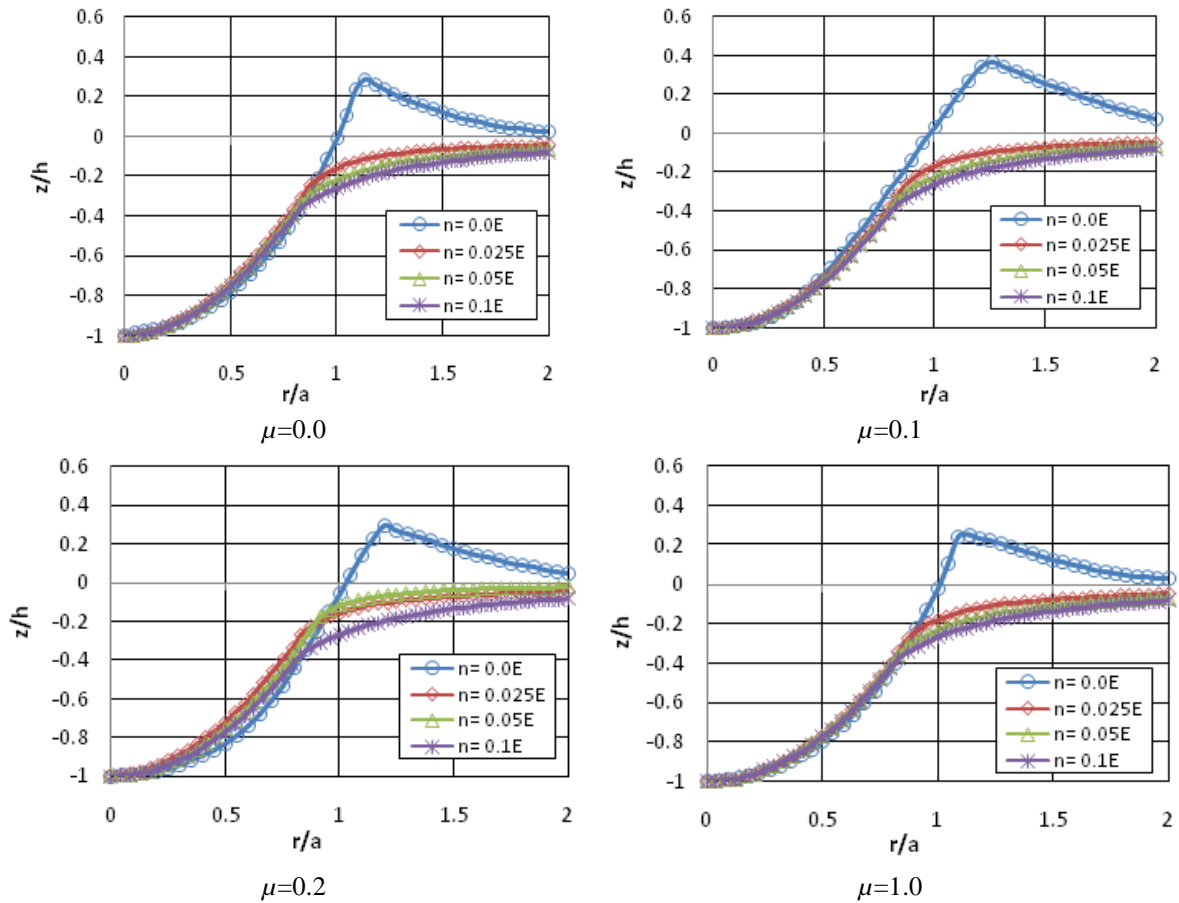


Fig. 12 Loaded Indentation profile for  $E/\sigma_y=1000$ ,  $h/R=0.2$  and  $\mu=0.0, \mu=0.1, \mu=0.2, \mu=1.0$

simulating the spherical indentation process of a material when depth of penetration is  $h/R=0.2$ ,  $E/\sigma_y=1000$  and the strain hardening exponent is 0. Fig. 11 shows that the pile up behaviour of the

material decreases as the value of coefficient of friction increases. The material with the coefficient of friction  $\mu=0$  has the greatest pile up behaviour and the material with coefficient of friction  $\mu=1.0$  has the least. This testifies that the pile up of a material is slightly dependent on its contact friction.

The pile up and sink in behaviour during loaded spherical indentation process is affected by the contact friction  $\mu$ . The loaded indentation profile is obtained for material with large  $E/\sigma_y=1000$  at  $h/R=0.2$  and different strain hardening exponents  $n=0.0E, 0.025E, 0.05E, 0.1E$ . From Fig. 12, the measurable amount of pile up and sink in for friction co-efficient  $\mu=0.0$  at different values of strain hardening exponent ( $n$ ) are obtained. The plot shows a plastic solid of  $n=0$  and three elastic/plastic solids of  $n=0.025, 0.05$  and,  $0.1$ . This simulation shows that the increase in strain hardening exponent ( $n$ ) of a material with any value of friction co-efficient ( $\mu$ ) results in decrease of piling up.

Fig. 12 also shows the behaviour of material for the coefficient of friction 0.1, 0.2 and 1.0 by varying the strain hardening exponent. From the profile, the pile up is observed in the plastic solid at  $n=0$  and sink in is observed in the three elastic solids having  $n=0.025, 0.05, 0.1$ . From the loaded indentation profiles of materials with varying contact friction  $\mu$ , it is observed that the change in pile up/ sink in behaviours are very less. But the change is evident from the profiles, as the amount of pile up obtained in a material decreases with increase in value of the contact friction  $\mu$ .

### 5. Experimental observations

Every material exhibits the different levels of isotropic hardening behaviour, so the analysis is compared with the multi-linear properties in order to correlate the obtained results to verify whether the consideration factors like strain hardening exponent ( $n$ ), yield stress ( $E/\sigma_y$ ), depth of penetration ( $h/R$ ) and, co-efficient of friction ( $\mu$ ) of a material helps to determine the exact magnitude of pile up or sink in behaviour during the spherical indentation process in ANSYS.

The properties for the materials like Mild steel, Brass, and Aluminium which have taken from the tensile testing tested by Shankar and Mayuram, 2008 is utilized for the analysis. The tested

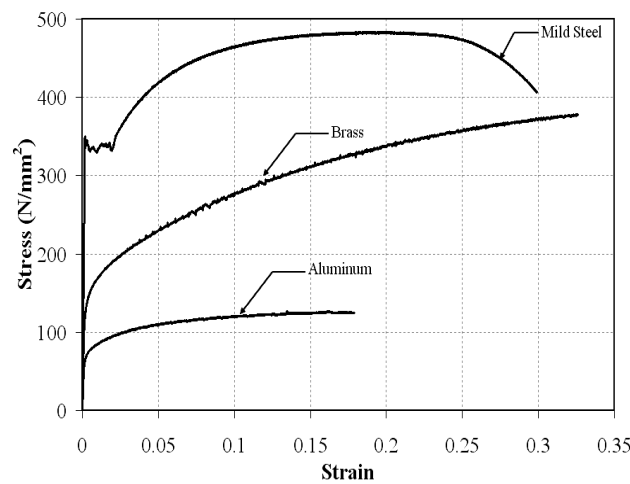


Fig. 13 Stress - strain curve (Shankar and Mayuram 2008)

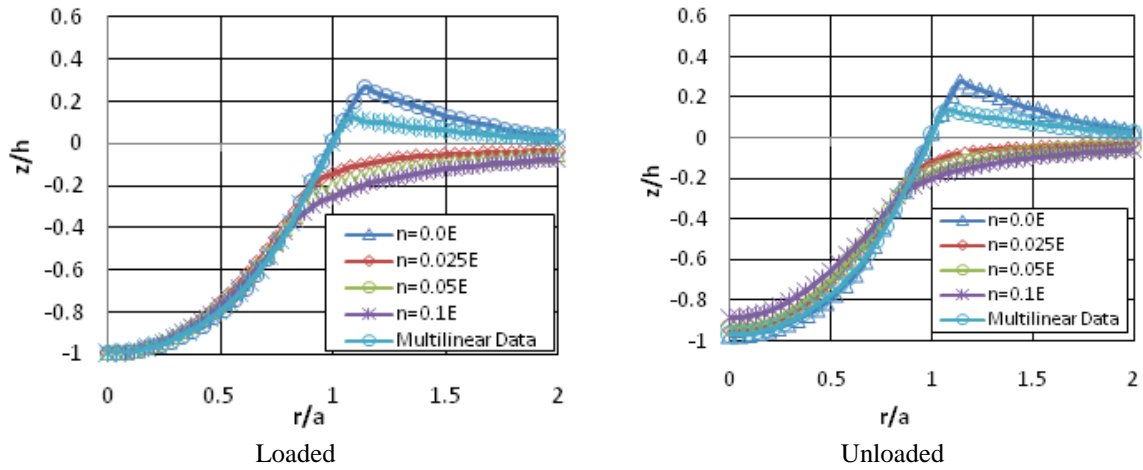


Fig. 14 Result comparison for mild steel at  $\sigma_y=340 \text{ N/mm}^2$ ,  $h/R=0.2$  and  $\mu=0.2$

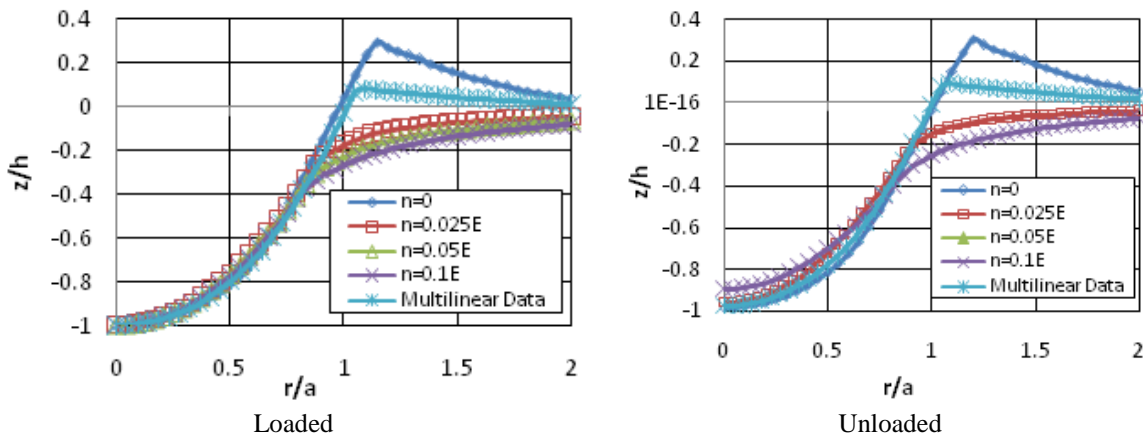


Fig. 15 Result comparison for brass at  $\sigma_y=139 \text{ N/mm}^2$ ,  $h/R=0.2$  and  $\mu=0.2$

results are directly incorporated in ANSYS to simulate the real multilinear behaviour. The stress-strain curve for these materials is shown in Fig. 13.

The correlation between the multi-linear data for different strain hardening exponents by considering other parameters as constant for the materials such as mild steel, brass and aluminium are shown in the Figs. 14-16 for the loading and unloading indentation profile. From the indentation profile, the magnitude of pile-up for the mild steel as well as aluminium is not exactly equal to obtained analysis data during loading and unloading given by Taljat and Pharr, 2004. It is inferred that the analysis data is closely resembles with the experimental data when the strain hardening exponent is in the range between  $0E$  to  $0.025E$ . Mostly practical materials exhibit a strain hardening coefficient value greater than  $0.0E$ , almost equal to  $0.01E$  but it varies depends on the material. For mild steel and aluminium, the results are matching closely to  $0.01E$  value and this result shows the importance of strain hardening parameter in the analysis. For the brass material the analysis data result closely matching with the experimental data when the strain hardening exponent is  $0.025E$  during loading as well as unloading process.

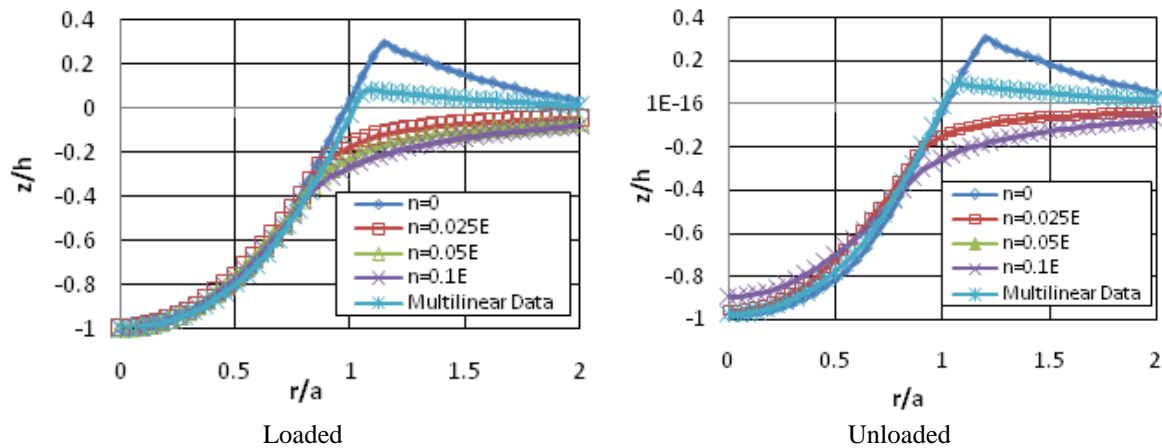


Fig. 16 Result comparison for aluminium at  $\sigma_y=71 \text{ N/mm}^2$ ,  $h/R=0.2$  and  $\mu=0.2$

## 6. Conclusions

The finite element concept is utilized to study the pile-up and sink-in behaviour for the wide range of materials with different Young's modulus, yield stresses, strain-hardening exponents and co-efficient of friction. The exact indentation model is created by using the two dimensional axisymmetrical model for simulating the indentation process on the lines of Taljat and Pharr (2004) work. The present study utilizes the effect of strain hardening behaviour on overall contact behaviour of a material. The results from the analysis suggest that the pile-up behaviour decreases with increase in the value of strain hardening exponent and thus escalating the sink-in behaviour and also the recovery of material increases with increase in the value of strain hardening exponent. The indentation profiles are greatly dependent not only on the strain hardening exponent but also dependent on the relative amount of plastic deformation as characterised by the ratio of the elastic modulus to yield stress ( $E/\sigma_y$ ), depth of penetration and friction co-efficient. The present analysis is also validated with the experimental data using the materials such as mild steel, brass and aluminium. From the analysis, the pile-up behaviour for mild steel and aluminium are closely resembles with the experimental data for the strain hardening exponent range  $0.01E$ . The pile-up behaviour for the brass is almost equal to the experimental data for the strain hardening exponent  $0.025E$ . From the extensive analysis, it is predicted that the strain hardening coefficient is an important parameter which should be considered for the indentation process.

## References

- Lin, D.C., Shreiber, D.I., Dimitriadis, E.K. and Horkay, F. (2009), "Spherical indentation of soft matter beyond the Hertzian regime: numerical and experimental validation of hyperelastic models", *Biomech. Model. Mech.*, **8**(5), 345-358.
- Lee, H.G., Lee, J.H. and Pharr, G.M. (2005), "A numerical approach to spherical indentation techniques for material property evaluation", *J. Mech. Phys. Solid.*, **53**(9), 2037-2069.
- Habbab, H., Mellor, B.G. and Syngellakis, S. (2006), "Post-yield characterisation of metals with significant pile-up through spherical indentation", *Acta Materialia*, **54**(7), 1965-1973.

- Hernot, X., Bartier, O., Bekouche, Y., El Abdi, R. and Mauvoisin, G. (2006), "Influence of penetration depth and mechanical properties on contact radius determination for spherical indentation", *Int. J. Solid. Struct.*, **43**(14), 4136-4153.
- Lee, J.H., Kim, T.H. and Lee, H.G. (2010), "A study on robust indentation techniques to evaluate elastic-plastic properties of metals", *Int. J. Solid. Struct.*, **47**(5), 647-664.
- Kucharski, S. and Mroz, Z. (2007), "Indentation of yield stress and plastic hardening parameters from a spherical indentation test", *Int. J. Mech. Sci.*, **49**(11), 1238-1250.
- Mata, M. and Alcala, J. (2004), "The role of friction on sharp indentation", *J. Mech. Phys. Solid.*, **52**(1), 145-165.
- Oliver, W.C. and Pharr, G.M. (1992), "Improved technique for determining hardness and elastic modulus using load and displacement sensing indentation experiments", *J. Mater. Res.*, **7**(6), 1564-1583.
- Poon, B., Rittel, D. and Ravichandran, G. (2008), "An analysis of nanoindentation in linearly elastic solids", *Int. J. Solid. Struct.*, **45**(24), 6018-6033.
- Pharr, G.M. (1998), "Measurement of mechanical properties by ultra-low load indentation", *Mater. Sci. Eng.*, **253**(1), 151-159.
- Shankar, S. and Mayuram, M.M. (2008), "Effect of strain hardening in elastic - plastic transition behavior in a hemisphere in contact with a rigid flat", *Int. J. Solid. Struct.*, **45**(10), 3009-3020.
- Mesarovic, S.D. and Fleck, N.A. (1999), "Spherical indentation of elastic-plastic solids", *Proc. Royal Soc.*, **455**(1987), 2707-2728.
- Taljat, B. and Pharr, G.M. (2004), "Development of pile-up during spherical indentation of elastic-plastic solids", *Int. J. Solid. Struct.*, **41**(14), 3891-3904.
- Yan, W., Sun, Q., Feng, X.Q. and Qian, L. (2007), "Analysis of spherical indentation of super elastic shape memory alloys", *Int. J. Solid. Struct.*, **44**(1), 1-17.
- Chen, X., Hutchinson, J.W. and Evans, A.G. (2005), "The mechanics of indentation induced lateral cracking", *J. Am. Ceramic Soc.*, **88**(5), 1233-1238.
- Wei, Y. and Hutchinson, J.W. (2003), "Hardness trends in micron scale indentation", *J. Mech. Phys. Solid.*, **51**(11), 2037-2056.